Table 2.5.3.13. *Wavevectors, point- and space-group symbols and CBED symmetries of one-dimensionally modulated crystals*

Wavevector transformation	Point-group symbol	Symmetry of incommensurate reflection	Space-group symbol	Dynamical extinction lines
$\mathbf{k} \rightarrow \mathbf{k}$	1	Same symmetry as average structure	1, s (1/2), t ($\pm$1/3), q ($\pm$1/4), h ($\pm$1/6)	Yes for s, q and h
$\mathbf{k} \rightarrow -\mathbf{k}$	$\bar{1}$	No symmetry	$\bar{1}$	No

reflections ought to show the symmetry of the average structure, while the incommensurate reflections lose the symmetry.

The problem of the finite size of the illuminated area is discussed using equations (2.5.3.7) and (2.5.3.8) in a paper by Terauchi & Tanaka (1993) and in the book by Tanaka *et al.* (1994, pp. 156–205). The results are as follows: Even if the size and position of an illuminated specimen area are changed, the intensity distribution in a CBED pattern changes but the symmetry of the pattern does not. To obtain the symmetries of incommensurate crystals, it is not necessary to take CBED patterns from an area whose diameter is larger than the period of the modulated structure. The symmetries of the modulated structure can appear when more than one unit cell of the average structure is illuminated for displacive modulations. For substitutional modulations, a specimen volume that produces the average atom form factor is needed, namely a volume of about 1 nm diameter area and 50 nm thick.

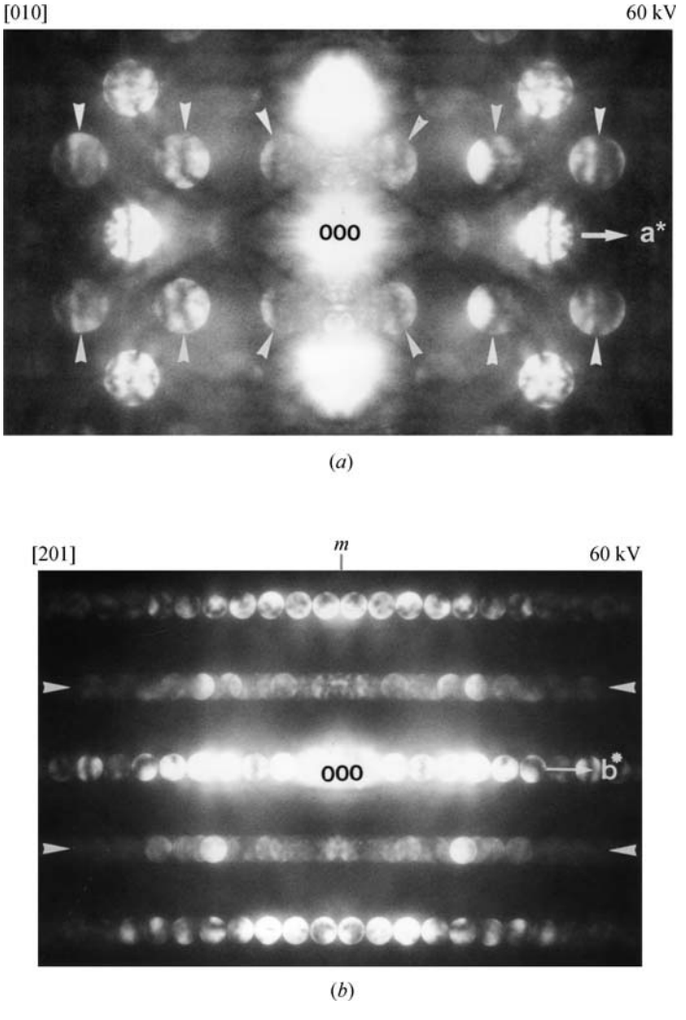

Fig. 2.5.3.19. CBED patterns of the incommensurate phase of $Sr_2Nb_2O_7$ taken at 60 kV. (*a*) [010] incidence: fundamental reflections show a mirror symmetry perpendicular to the a^* axis but incommensurate reflections do not [symmetry ($^m_1$)]. (*b*) [201] incidence: incommensurate reflections show mirror symmetry perpendicular to the b^* axis [symmetry ($^m_1$)]. The wave number vector of the modulation is $\mathbf{k} = (\frac{1}{2} - \delta)\mathbf{a}^*$.

Table 2.5.3.13 shows the point-group symmetries (third column) of the incommensurate reflections for the two point-group subsymbols. For symmetry subsymbol 1, both the fundamental and incommensurate reflections show the symmetries of the average structure. For symmetry subsymbol $\bar{1}$, the fundamental reflections show the symmetries of the average structure but the incommensurate reflections do not have any symmetry. These facts imply that the symmetries of the incommensurate reflections are determined by the point group of the average structure and the modulation wavevector **k**. In other words, observation of the symmetries of the incommensurate reflections is not necessary for the determination of the point groups, although it can ascertain the point groups of the modulated crystals.

An example of point-group determination is shown for the incommensurate phase of $Sr_2Nb_2O_7$. Many materials of the $A_2B_2O_7$ family undergo phase transformations from space group $Cmcm$ to $Cmc2_1$ and further to $P2_1$ with decreasing temperature. An incommensurate phase appears between the $Cmc2_1$ phase and the $P2_1$ phase. $Sr_2Nb_2O_7$ transforms at 488 K from the $Cmc2_1$ phase into the incommensurate phase with a modulation wavevector $\mathbf{k} = (\frac{1}{2} - \delta)\mathbf{a}^*$ (δ = 0.009–0.023) but does not transform into the $P2_1$ phase. The space group of $Sr_2Nb_2O_7$ was reported as $P^{C\,mc2_1}_{\bar{1}s\bar{1}}$ (Yamamoto, 1988). (Since the space-group notation $Cmc2_1$ is broadly accepted, the direction of the modulation is taken as the a axis.) The point group of the phase is $^{mm2}_{\bar{1}\,1\,\bar{1}}$. The modulation wavevector **k** is transformed to $-\mathbf{k}$ by the mirror symmetry operation perpendicular to the a axis ($^m_1$) and by the twofold rotation symmetry operation about the c axis ($^2_1$). The wavevector is transformed into itself by the mirror symmetry operation perpendicular to the b axis ($^m_1$).

Fig. 2.5.3.19(*a*) shows a CBED pattern of the incommensurate phase of $Sr_2Nb_2O_7$ taken with the [010] incidence at an accelerating voltage of 60 kV. The reflections indicated by arrowheads are the incommensurate reflections. Other reflections are the fundamental reflections. Since the pattern is produced by the interaction of the reflections in the zeroth-order Laue zone, symmetry operations ($^m_1$) and ($^2_1$) act the same. These symmetries are confirmed by the fact that the fundamental reflections show mirror symmetry perpendicular to the a^* axis (twofold rotation symmetry about the c^* axis) but the incommensurate reflections do not. Fig. 2.5.3.19(*b*) shows a CBED pattern of the incommensurate phase of $Sr_2Nb_2O_7$ taken with the [201] incidence at 60 kV. The reflections in the two rows indicated by arrowheads are the incommensurate reflections and the others are the fundamental reflections. Symmetry symbol ($^m_1$) implies that both the fundamental and incommensurate reflections display mirror symmetry perpendicular to the b^* axis. Fig. 2.5.3.19(*b*) exactly exhibits the symmetry.

2.5.3.4.3. Space-group determination

Table 2.5.3.13 shows the space-group symbols (fourth column) of the modulated crystals. When a glide (screw) component τ_4 between the modulation waves of two atom rows is 0, 1/2, $\pm$1/3, $\pm$1/4 or $\pm$1/6, symbol 1, s, t, q or h is given, respectively (de Wolff *et al.*, 1981). Such glide components are allowed for point-group symmetry 1 but are not for point-group symmetry $\bar{1}$. Dynamical

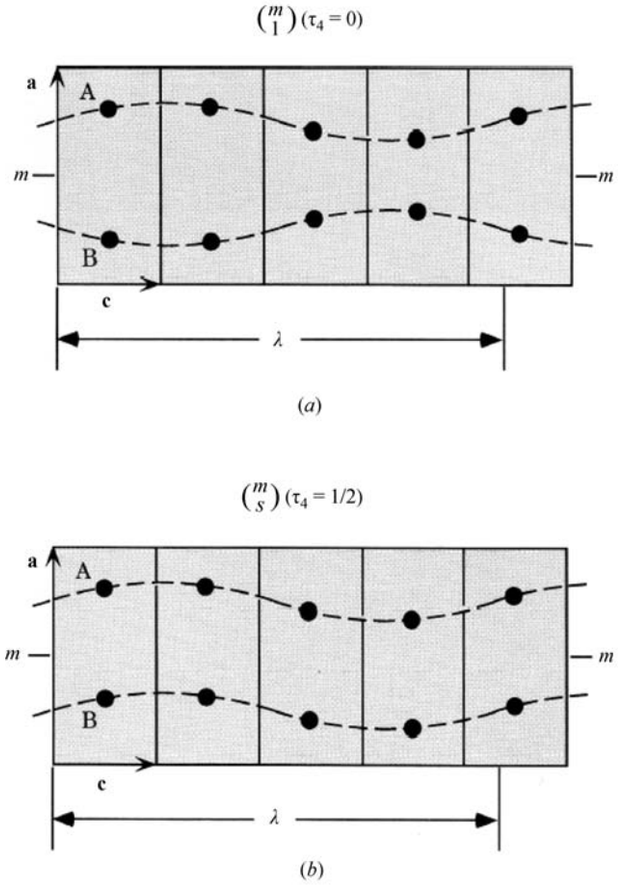

Fig. 2.5.3.20. (*a*) Mirror symmetry of modulation waves $\binom{m}{1}$ $\tau_4 = 0$. (*b*) Glide symmetry of modulation waves $\binom{m}{s}$ $\tau_4 = \frac{1}{2}$. The wave number vector of modulation is $k_3\mathbf{c}^*$.

extinction occurs for glide components *s*, *q* and *h* but does not for glide component *t*. When the average structure does not have a glide component, dynamical extinction due to a glide component τ_4 appears in odd-order incommensurate reflections. When the average structure has a glide component, dynamical extinction due to a glide component τ_4 appears in incommensurate reflections with $h_i + h_4 = 2n + 1$, where h_i and h_4 are the reflection indices for the average structure and incommensurate structure, respectively. Details are given in the paper by Terauchi *et al.* (1994).

Fig. 2.5.3.20(*a*) illustrates mirror symmetry $\binom{m}{1}$ between atom rows A and B, which is perpendicular to the *b* axis with no glide component ($\tau_4 = 0$). Here, the wave number vector of the modulation is assumed to be $\mathbf{k} = k_3\mathbf{c}^*$ following the treatment of de Wolff *et al.* (1981). Fig. 2.5.3.20(*b*) illustrates glide symmetry $\binom{m}{s}$ with a glide component $\tau_4 = \frac{1}{2}$. The structure factor $F(h_1h_2h_3h_4)$ is written for the glide plane $\binom{m}{s}$ of an infinite incommensurate crystal as

$$\begin{aligned}
&F(h_1h_2h_3h_4)\\
&= \sum_{\mu=1}^{N} f_\mu \exp[2\pi i(h_1\bar{x}_1^\mu + h_2\bar{x}_2^\mu + h_3\bar{x}_3^\mu)]\\
&\quad \times \int_0^1 \exp\{2\pi i[h_1u_1^\mu + h_2u_2^\mu + (h_3 + h_4k_3)u_3^\mu + h_4\bar{x}_4^\mu]\}\,\mathrm{d}\bar{x}_4^\mu\\
&\quad + \exp(h_4\pi i)\sum_{\mu=1}^{N} f_\mu \exp[2\pi i(h_1\bar{x}_1^\mu - h_2\bar{x}_2^\mu + h_3\bar{x}_3^\mu)]\\
&\quad \times \int_0^1 \exp\{2\pi i[h_1u_1^\mu - h_2u_2^\mu + (h_3 + h_4k_3)u_3^\mu + h_4\bar{x}_4^\mu]\}\,\mathrm{d}\bar{x}_4^\mu.
\end{aligned} \tag{2.5.3.10}$$

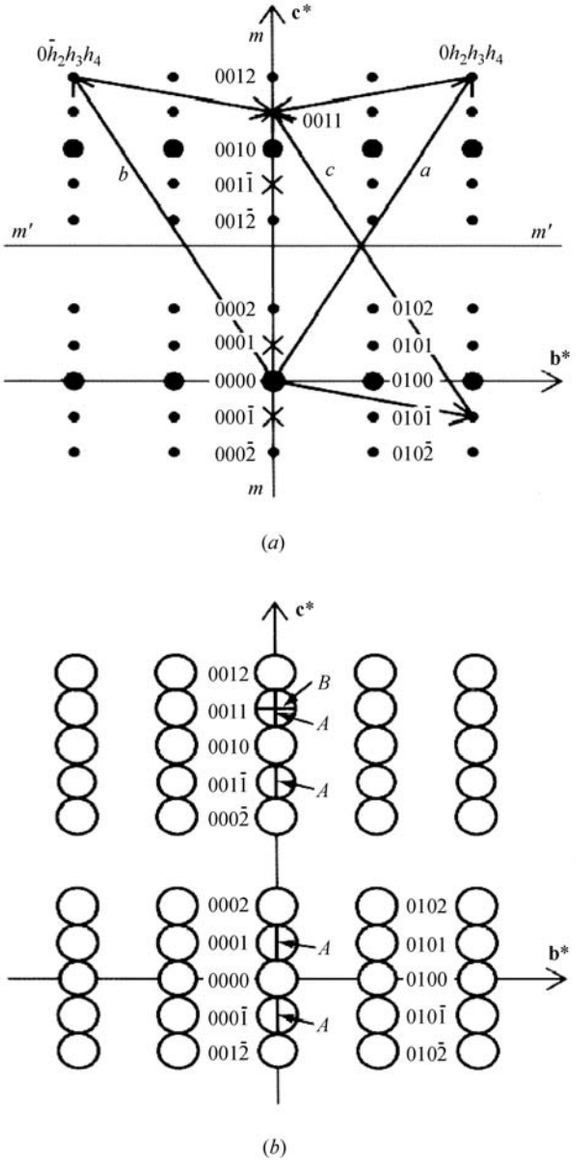

Fig. 2.5.3.21. (*a*) *Umweganregung* paths *a*, *b* and *c* to the 0011 forbidden reflection. (*b*) Expected dynamical extinction lines are shown, the 0011 reflection being excited. The wave number vector of modulation is $k_3\mathbf{c}^*$.

Thus, the following phase relations are obtained between the two structure factors:

$$\begin{aligned}
F(h_1h_2h_3h_4) &= F(h_1\bar{h}_2h_3h_4) \quad \text{for } h_4 \text{ even},\\
F(h_1h_2h_3h_4) &= -F(h_1\bar{h}_2h_3h_4) \quad \text{for } h_4 \text{ odd}.
\end{aligned} \tag{2.5.3.11}$$

These relations are analogous to the phase relations between the two structure factors for an ordinary three-dimensional crystal with a glide plane. The relations imply that dynamical extinction occurs for the glide planes and screw axes of the (3 + 1)-dimensional crystal with an infinite dimension along the direction of the incommensurate modulation wavevector **k**. Terauchi *et al.* (1994) showed that approximate dynamical extinction occurs for an incommensurate crystal of finite dimension.

Fig. 2.5.3.21(*a*) and (*b*) illustrate a spot diffraction pattern and a CBED pattern, respectively, expected from a modulated crystal with a (3 + 1)-dimensional space group $P^{P2mm}_{\bar{1}s\bar{1}}$ ($\mathbf{k} = k_3\mathbf{c}^*$) at the [100] incidence. The large and small spots in Fig. 2.5.3.21(*a*) designate the fundamental ($h_4 = 0$) and incommensurate reflections ($h_4 \neq 0$), respectively. The $00h_3h_4$ (h_4 = odd) reflections

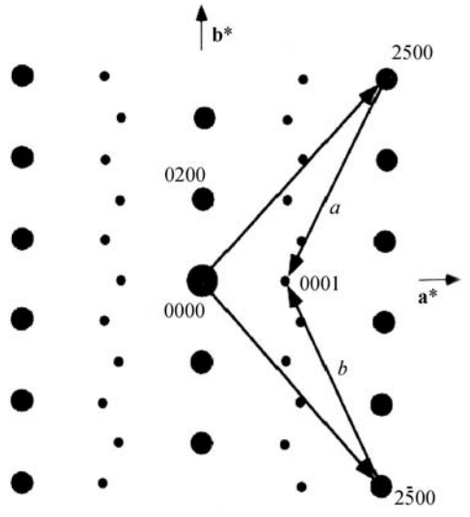

Fig. 2.5.3.22. Schematic diffraction pattern at the [001] incidence of $Sr_2Nb_2O_7$. *Umweganregung* paths *a* and *b via* fundamental reflections to the 0001 incommensurate reflection. Large and small spots denote fundamental and incommensurate reflections, respectively. The wave number vector of modulation is $\mathbf{k} = (\frac{1}{2} - \delta)\mathbf{a}^*$.

shown by crosses are kinematically forbidden by the glide plane (^m_s) perpendicular to the *b* axis. *Umweganregung* paths *a*, *b* and *c* in the ZOLZ to a kinematically forbidden reflection are drawn. The two paths *a* and *b* are geometrically equivalent with respect to the line *m*–*m* perpendicular to the *b* axis. Since every *Umweganregung* path to a kinematically forbidden reflection contains an odd number of $F(0h_{2,i}h_{3,i}h_{4,i})$ with odd $h_{4,i}$, the following equation is obtained.

$$F(0h_{2,1}h_{3,1}h_{4,1})F(0h_{2,2}h_{3,2}h_{4,2})\ldots F(0h_{2,n}h_{3,n}h_{4,n}) \quad \text{for path } a$$
$$= -F(0\bar{h}_{2,1}h_{3,1}h_{4,1})F(0\bar{h}_{2,2}h_{3,2}h_{4,2})\ldots F(0\bar{h}_{2,n}h_{3,n}h_{4,n})$$
$$\text{for path } b, \qquad (2.5.3.12)$$

where $\sum_{i=1}^{n} h_{2,i} = 0$, $\sum_{i=1}^{n} h_{3,i} = h_3$ and $\sum_{i=1}^{n} h_{4,i} = h_4$ (h_4 = odd).

When reflection $00h_3h_4$ (h_4 = odd) is exactly excited, the two paths *a* and *c* are symmetric with respect to the bisector m'–m' of the diffraction vector of the reflection and have the same excitation error. The waves passing through these paths have the same amplitude but different signs. Thus the following relation is obtained.

$$F(0h_{2,1}h_{3,1}h_{4,1})F(0h_{2,2}h_{3,2}h_{4,2})\ldots F(0h_{2,n}h_{3,n}h_{4,n}) \quad \text{for path } a$$
$$= -F(0\bar{h}_{2,n}h_{3,n}h_{4,n})F(0\bar{h}_{2,n-1}h_{3,n-1}h_{4,n-1})\ldots F(0\bar{h}_{2,1}h_{3,1}h_{4,1})$$
$$\text{for path } c, \qquad (2.5.3.13)$$

where $\sum_{i=1}^{n} h_{2,i} = 0$, $\sum_{i=1}^{n} h_{3,i} = h_3$ and $\sum_{i=1}^{n} h_{4,i} = h_4$ (h_4 = odd).

Therefore, dynamical extinction occurs in kinematically forbidden reflections of incommensurate crystals. Fig. 2.5.3.21(*b*) schematically shows the extinction lines in odd-order incommensurate reflections, where the 0011 reflection is exactly excited.

We consider the dynamical extinction from $Sr_2Nb_2O_7$ whose space group is $P^{Cmc2_1}_{\bar{1}\,s\,\bar{1}}$. The glide plane (^c_s) is perpendicular to the *b* axis with a glide vector $(\mathbf{c} + \mathbf{a}_4)/2$. The wave number vector of the modulation is $\mathbf{k} = (\frac{1}{2} - \delta)\mathbf{a}^*$. (Since space-group notation $Cmc2_1$ is broadly accepted, the direction of the modulation is taken as the *a* axis.) The reflections $h_10h_3h_4$ with $h_3 + h_4 = 2n + 1$ (n = integer) are kinematically forbidden. Fig. 2.5.3.22 shows a schematic diffraction pattern of $Sr_2Nb_2O_7$ at the [001] incidence. The large

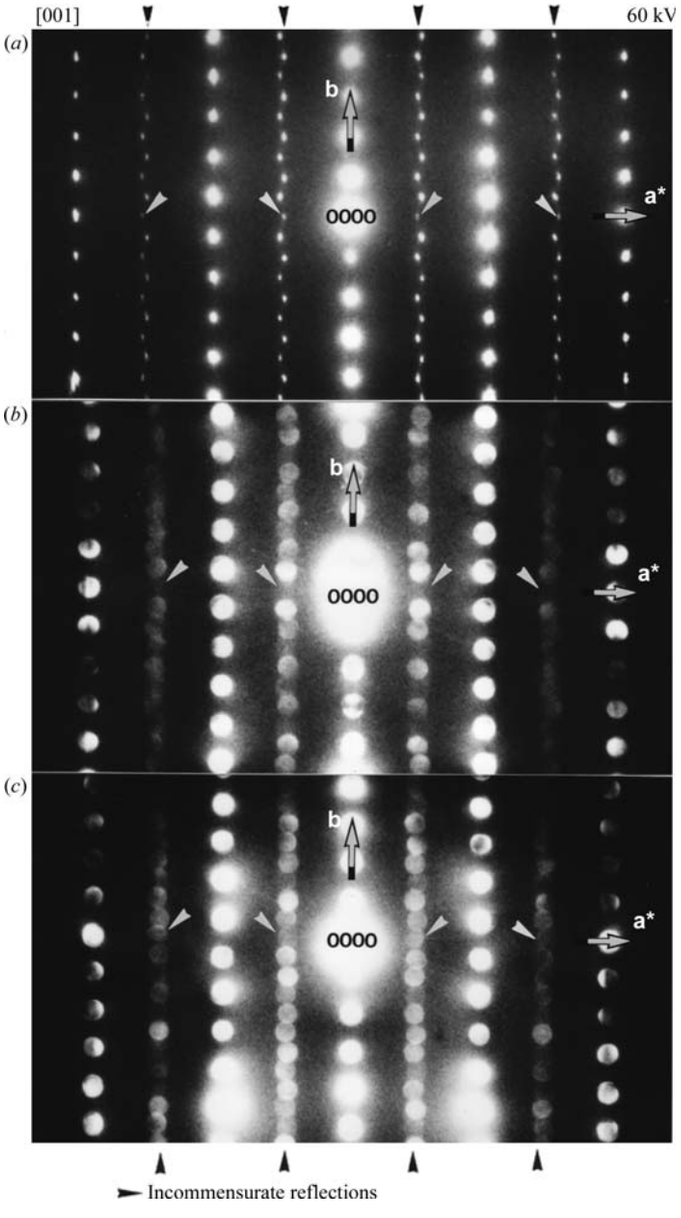

Fig. 2.5.3.23. Diffraction pattern of $Sr_2Nb_2O_7$ taken with [001] incidence at 60 kV. (*a*) Spot diffraction pattern. Kinematically forbidden 0001 and 200$\bar{1}$ incommensurate reflections exhibit definite intensity. (*b*) Zone-axis CBED pattern showing dynamical absence of 0001 and 200$\bar{1}$ incommensurate reflections. (*c*) CBED pattern taken at an incidence with a small tilt from the zone axis to the *b** direction. The kinematically forbidden incommensurate reflections have intensity due to incomplete cancellation of two waves through the *Umweganregung* paths. The wave number vector of modulation is $\mathbf{k} = (\frac{1}{2} - \delta)\mathbf{a}^*$.

and small spots indicate the fundamental (h_4 = 0) and incommensurate ($h_4 \neq 0$) reflections, respectively. *Umweganregung* paths *a* and *b* to the kinematically forbidden 0001 reflection *via* a fundamental reflection in the ZOLZ are drawn.

Fig. 2.5.3.23(*a*) shows a spot diffraction pattern of the incommensurate phase of $Sr_2Nb_2O_7$ taken with the [001] incidence at 60 kV. The incommensurate reflections in which dynamical extinction lines appear at this incidence are those with the indices $h_{1,\text{even}}00h_{4,\text{odd}}$ because $h_3 = 0$ and $h_1 + h_2 = 2n$ due to the lattice type *C* of the average structure.

The reflections in the four columns indicated by black arrowheads are incommensurate reflections. The reflections 0001, 000$\bar{1}$, 200$\bar{1}$ and $\bar{2}$001 designated by white arrowheads are kinematically forbidden but exhibit certain intensities, which are caused by multiple diffraction. Other reflections are fundamental reflections due to the average structure.

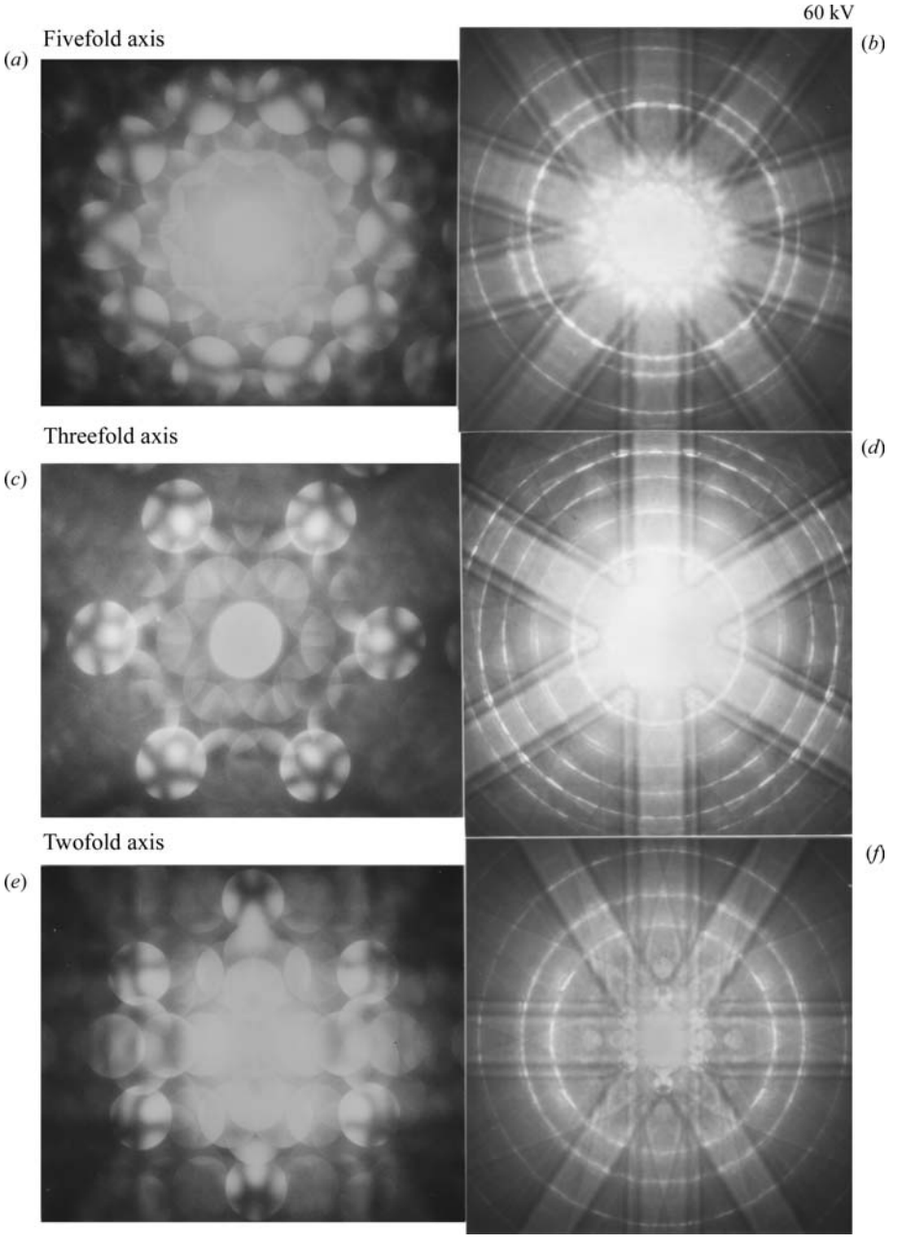

Fig. 2.5.3.24. Three pairs of ZOLZ [(*a*), (*c*) and (*e*)] and HOLZ [(*b*), (*d*) and (*f*)] CBED patterns taken at 60 kV from an area of $Al_{74}Mn_{20}Si_6$ about 3 nm in diameter and about 10 nm thick (Tanaka, Terauchi, Suzuki *et al.*, 1987). Symmetries are (*a*) 10*mm*, (*b*) 5*m*, (*c*) 6*mm*, (*d*) 3*m*, (*e*) 2*mm* and (*f*) 2*mm*.

Fig. 2.5.3.23(*b*) shows a CBED pattern corresponding to Fig. 2.5.3.23(*a*), taken from a specimen area 3 nm in diameter. The excitation errors of two *Umweganregung* paths *a* and *b* are the same at this electron incidence. The reflections 0001, $000\bar{1}$, $200\bar{1}$ and $\bar{2}001$ indicated by white arrowheads show no intensity. Dynamical extinction does not appear as a line in the present case because the width of the extinction line exceeds the disc size of the reflections. Fig. 2.5.3.23(*c*) shows a CBED pattern taken at an incidence slightly tilted toward the b^* axis from that for Fig. 2.5.3.23(*b*) or the [001] zone-axis incidence. The excitation errors are no longer the same for the two *Umweganregung* paths. Thus, it is seen that the kinematically forbidden reflections indicated by white arrowheads have intensities due to incomplete cancellation of waves coming through different paths, which is an additional proof of the dynamical extinction.

2.5.3.5. Symmetry determination of quasicrystals

2.5.3.5.1. Icosahedral quasicrystals

Penrose (1974) demonstrated that a two-dimensional plane can be tiled with thin and fat rhombi to give a pattern with local fivefold rotational symmetries but with no translational symmetry. Mackay (1982) extended the tiling to three dimensions using acute and obtuse rhombohedra, which also resulted in the acquisition of local fivefold rotational symmetries and in a lack of translational symmetry. The three-dimensional space-filling method was later completed by Ogawa (1985). These studies, however, remained a matter of design or geometrical amusement until Shechtman *et al.* (1984) discovered an icosahedral symmetry presumably with long-range structural order in an alloy of Al_6Mn (nominal composition) using electron diffraction. Since then, the term quasicrystalline order, a new class of structural order with no translational symmetry but long-range structural order, has been coined. Levine & Steinhardt (1984) showed that the quasilattice produces sharp diffraction patterns and succeeded in reproducing almost exactly the diffraction pattern obtained by Shechtman *et al*. (1984) using the Fourier transform of a quasi-periodic icosahedral lattice. When analysing X-ray and electron-diffraction data for a quasicrystal, the diffraction peaks can be successfully indexed by six independent vectors pointing to the vertices of an icosahedron. It was then found that the icosahedral quasicrystal can be described in terms of a regular crystal in six